Synthesis and Characterization of CL-PA Ionic Liquid

Ali Tuğrul Albayrak[*]

[*]Istanbul University-Cerrahpaşa, Faculty of Engineering, Department of Chemical Engineering, Istanbul, Avcilar, 34320, Türkiye

Abstract: Caprolactam is most commonly used in the production of Nylon 6 in industry and is generally produced from cyclohexanone by the Beckmann rearrangement. Orthophosphoric acid is generally used in fertilizer production and is produced through two processes: wet and dry. In this study, detailed characterization of CL-PA was carried out by synthesizing CL-PA ionic liquid from orthophosphoric acid (PA) and caprolactam (CL). FTIR, Raman and UV-Vis spectroscopic analyses reveal that a bond is formed between CL and PA. The thermal behavior of CL-PA ionic liquid was inspected by TGA and DSC. It has been observed that the decomposition temperature of CL-PA ionic liquid is different from that of the starting materials (CL and PA). It was disclosed by DSC analysis that CL-PA ionic liquid only has a glass transition temperature. The room-temperature CL-PA ionic liquid synthesized from solid CL with melting point of 70.34 ℃ and 85 wt.% PA did not show any melting or freezing point and the glass transition temperature was found to be -27 ℃. It was revealed that CL-PA ionic liquid was more thermally stable than CL which alone almost completely evaporated at about 197 ℃. As a result of FTIR analysis of CL-PA ionic liquid and its constituents, it was demonstrated that –NH peaks of CL disappeared in the CL-PA spectrum and the peak of C=O group shifted to a lower frequency (i.e., 1604 cm^{-1}). In the Raman analysis of CL-PA and its constituents, it was observed that the asymmetric C=O bending vibration and C=O stretching vibration of CL disappeared in the CL-PA spectrum. In the UV spectrum, it was observed that the maximum absorbance of CL-PA ionic liquid varied with respect to that of CL.

1. INTRODUCTION

ε-Caprolactam is a water-soluble lactam (Kalinová et al., 2016) with a molecular formula of $C_6H_{11}NO$ (Cherkasova et al., 2009) and a melting point of 69 ℃ (Kabo et al., 1992). Caprolactam is produced mostly from cyclohexanone by using NH_2OH and then H_2SO_4 (Beckmann Rearrangement) (McGraw-Hill Concise Encyclopedia of Science & Technology, 2005). However, the Beckmann rearrangement has disadvantages such as corrosion of the reactor by sulfuric acid and the formation of large amounts of ammonium sulfate as waste product (You et al., 2008). Therefore, alternative methods for the Beckmann Rearrangement have been proposed. In a study (S. Sun et al., 2022) in which the deep eutectic solvent Choline Chloride-Trifluoromethanesulphonic Acid [ChCl][TfOH]$_3$ was synthesized as catalyst and reaction medium, ε-caprolactam was obtained with

98.8% yield and 100% conversion of cyclohexanone oxime at the end of a 2-hour Beckmann rearrangement at 100 ℃ in the presence of [ChCl][TfOH]$_3$ and it has been reported that the [ChCl][TfOH]$_3$ recovered after the reaction can be reused consecutive seven times without significantly losing its activity (the caprolactam yield obtained after the 7th reuse is up to 98%). In another study (Ren et al., 2023), Bronsted acidic caprolactam-methanesulfonic acid [CPL][2MSA] ionic liquid was synthesized as a catalyst, and as a result of a 2-hour liquid phase Beckmann rearrangement at 90 ℃, caprolactam was obtained with 100% conversion and 95% selectivity and it has been reported that under optimal conditions, [CPL][2MSA] can be reused ten times for CL synthesis. A review on the use of zeolite catalysts for the environmentally friendly manufacturing process of CL has also been published (H. Wang et al., 2023). Caprolactam is generally used in the production of Nylon 6 (Mather & Wardman,

2015). The previously mentioned and other CL synthesis methods, including their advantages and disadvantages, are briefly summarized in Table 1. As can be seen from the table, in addition to the importance of high conversion and high selectivity for the reaction, low temperatures and low pressures are particularly more favorable in terms of cost.

Orthophosphoric acid is usually available as 85 wt.% viscous aqueous solutions (House, 2020). Orthophosphoric acid has three different pK_a values (pK_{a1} = 2.15, pK_{a2} = 7.21 and pK_{a3} = 12.36) in water (Lange & Speight, 2005). Pure orthophosphoric acid is an inorganic acid with a melting point of 42.35 ℃ (Ashurst, 2016) . H_3PO_4 is produced by two methods: wet process (Benvenuto & Plaumann, 2021), which involves the reaction of phosphate-containing

minerals with sulfuric acid, and dry process (L. K. Wang, 2006), which involves the reaction of diphosphorus pentoxide with water. Orthophosphoric acid is generally used in fertilizer production (Gilmour, 2014). Biochars are chemically activated with orthophosphoric acid to increase their adsorption capacity (Chu et al., 2018). In a study (Chen et al., 2019) in which biochar prepared using chicken feathers was activated with orthophosphoric acid, it was reported that the adsorption of Cd^{2+} and Pb^{2+} ions was further increased by orthophosphoric acid-modified biochar. There are also other applications of orthophosphoric acid, such as the use of orthophosphoric acid in fuel cells (Q. Sun et al., 2021).

Table 1: Some synthesis methods of caprolactam.

Materials	Reaction Conditions	Advantages	Disadvantages	Reference
Cyclohexanone Oxime, [ChCl][TfOH]₃ as DES	100 ℃, 2 hours	Reusability of DES, low reaction time, easy recovery of DES, high CL yield (98.8%), 100% conversion of cyclohexanone oxime, No $(NH_4)_2SO_4$		(S. Sun et al., 2022)
Cyclohexanone Oxime, [CPL][2MSA] as Ionic Liquid	90 ℃, 2 hours	High conversion (100%) and high CL selectivity (95%), Reusability of Ionic Liquid, No $(NH_4)_2SO_4$, environmentally friendly ionic liquid catalyst		(Ren et al., 2023)
Cyclohexanone Oxime, MFI zeolite catalyst	280 – 400 ℃	High CL conversion, high CL selectivity, no $(NH_4)_2SO_4$	High temperature, catalyst requirement with high thermal stability	(Ichihashi et al., 2003; W.-C. Li et al., 2005)
Aqueous solution of cyclohexanone oxime, Supercritical Water	673 K and 40 MPa	CL yield > 80% CL selectivity of 100% No $(NH_4)_2SO_4$	High temperature and high pressure	(Sato et al., 2005)
SNIA viscosa Process, toluene as starting materials, air, hydrogen, nitrosyl sulfuric acid in the presence of oleum	The first step: Co catalyst, 160-170 ℃, 8–10 bar The second step: Pd-on-graphite catalyst, 170 ℃, 10–17 bar The third step: 80 ℃	72% CL yield 90% CL selectivity ammonium sulfate-free sythesis	High temperature and high pressure in the first two consecutive steps	(Maxwell, 2005)

In addition to the application areas of orthophosphoric acid and caprolactam on their own, they have also been used in the preparation of deep eutectic solvents and ionic liquids. Deep eutectic solvents, consisting of a hydrogen bond donor and a

hydrogen bond acceptor, and ionic liquids, composed of an organic cation and an inorganic or organic anion (Płotka-Wasylka et al., 2020), have many advantages (Bajpai, 2021) such as low volatility, wide liquid range, high thermal stability and the

capacity to dissolve inorganic and organic substances.

CL-based ionic liquids have been used in the removal of H_2S (Guo et al., 2011), absorption of SO_2 (Liu et al., 2013), oxidative desulfurization (Yang et al., 2016), and lipid recovery from microalgae (Naiyl et al., 2022). CL-based deep eutectic solvents have applications such as oxidative desulfurization of diesel fuel (Hao et al., 2018), natural gas desulfurization (Karibayev & Shah, 2020), extractive desulfurization of diesel fuel (L. Xu et al., 2022), use as electrolyte in energy storage systems (S. Wang et al., 2024; C. Xu et al., 2019), and isolation and recovery of valuable metals such as lithium and cobalt from waste lithium-ion batteries (Cao et al., 2023). Besides, in a study (Celik et al., 2021) in which caprolactam-glycine was synthesized, it was

reported that this substance has an antibacterial effect. Proton transfer in orthophosphoric acid-trimethyl amine, orthophosphoric acid-imidazole, orthophosphoric acid-lidocaine and orthophosphoric acid-creatinine protic ionic liquids was investigated in detail using Gaussian 09 software and it has been demonstrated that unhindered proton transfer occurs in the orthophosphoric acid-creatinine ionic liquid (Zhu et al., 2020). In a study (Zhang et al., 2023) examining the recovery of metals from waste lithium-ion batteries, it was determined that while the recovery of lithium and cobalt in the first cycle was 100 and 92.8%, respectively, these recoveries were 94.3 and 80.8%, respectively, after the fifth cycle.

In this study, CL-PA ionic liquid was synthesized and its characterization was inspected in detail.

2. EXPERIMENTAL SECTION

2.1. Materials
85 wt.% orthophosphoric acid aqueous solution from Balmumcu Kimya, 99 wt.% caprolactam and ≥ 99 wt.% dichloromethane (as solvent) from Sigma-Aldrich were provided.

2.2. Synthesis
0.25 mol of caprolactam was placed in a 250-mL conical flask and dissolved in 50 mL of

dichloromethane. 0.25 mol of orthophosphoric acid was added dropwise to the caprolactam solution in the flask immersed in a salt water bath below 0 ℃ and stirring was continued for 30 min below 0 ℃. Then, stirring was carried out at room temperature for 24 h. Dichloromethane and water were removed from the ionic liquid at 60 ℃ and 40 mbar under vacuum using a rotary evaporator. A transparent and colorless viscous ionic liquid was obtained at room temperature. The synthesis reaction of CL-PA is shown in Scheme 1.
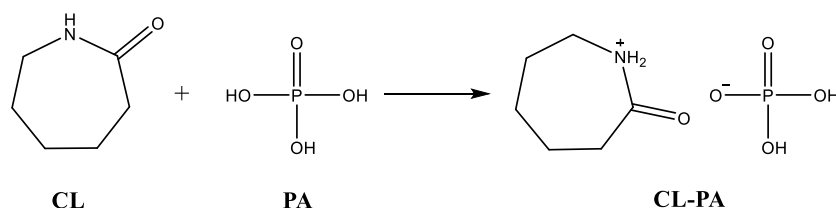
Scheme 1. Synthesis of CL-PA ionic liquid.

3. RESULTS AND DISCUSSION

3.1. DSC (Differential Scanning Calorimetry) Analysis
Thermal analysis was performed by Mettler Toledo DSC 3+. To observe the thermal behavior, CL-PA ionic liquid was cooled from 150 to −100 ℃ at a rate of 10 ℃/min under nitrogen flow and then heated from −100 to 150 ℃ at the same rate. As a result of the DSC analysis, as seen in Figure 1, no freezing point was observed in the ionic liquid and the glass transition temperature from the heating cycle was determined as −27 ℃.

Thermal analysis of CL was performed by TA Instruments DSC250. CL was first heated from 20 to 150 ℃ at a rate of 5 ℃/min under nitrogen flow, and then cooled from 150 to 0 ℃ at the same rate. As seen in Figure 2, the melting point taken as the peak temperature on the heating cycle was determined as

70.34 ℃, and 41.44 ℃, taken as the peak temperature on the cooling cycle, was possibly considered the crystallization temperature.

3.2. TGA (Thermogravimetric Analysis)
Thermogravimetric analysis of CL-PA ionic liquid and CL was performed by Mettler Toledo DSC 3+. The ionic liquid was heated from 25 to 700 ℃ at a rate of 10 ℃/min under nitrogen atmosphere. In Figure 3, in the first region up to 163 ℃, the remaining water in CL-PA ionic liquid completely evaporated and CL also started to separate from the ionic liquid (Fang et al., 2018). In the second region between 163-217 ℃, CL was completely separated and orthophosphoric acid began to decompose into pyrophosphoric acid (Yankova & Tankov, 2021). In the third region at 217-420 ℃, thermal degradation of orthophosphoric acid to pyrophosphoric acid is completed.
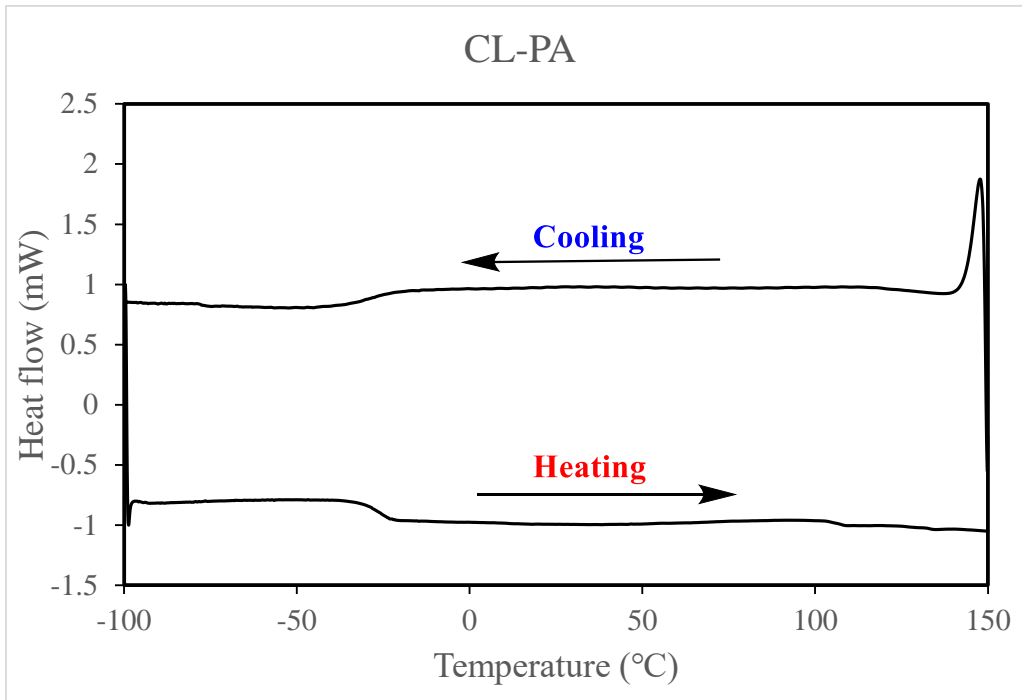
CL-PA

Figure 1. DSC thermal analysis of CL-PA ionic liquid.
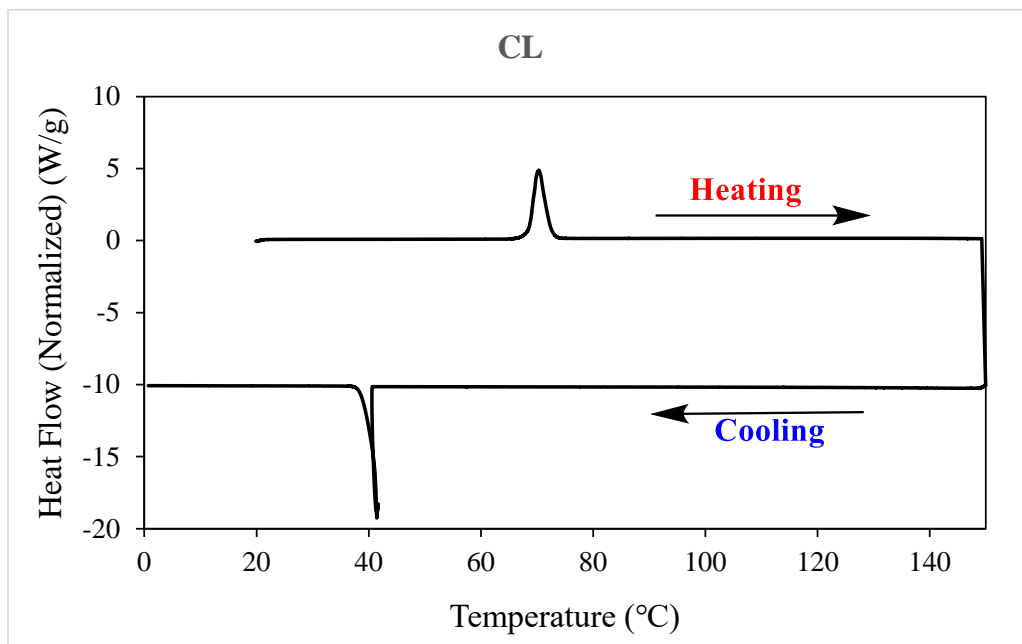
CL

Figure 2. DSC thermal analysis of CL.

3.3. FTIR (Fourier Transform Infrared) Analysis

FTIR analysis of CL-PA ionic liquid was carried out by JASCO FT/IR-4700 in the range of 4000–400 cm^{-1}. The resolution and the number of scans as FTIR operating parameters is 4 cm^{-1} and 16, respectively. When the spectrum of 85 wt% orthophosphoric acid aqueous solution is examined in Figure 4, the peaks at 2777, 1635, 1111, 952 and 875 cm^{-1} are assigned to the intermolecular hydrogen bonding interaction of H$_3$PO$_4$, the bending vibration of the –OH bond, the stretching vibration of P=O bond, the asymmetric stretching vibration of P–OH bond, and the symmetric stretching vibration of P–OH bond, respectively (Wei et al., 2020). The peak at 3550 cm^{-1} indicates the presence of water (Malek & Chong, 2000). In the CL spectrum, the peaks at 3295, 3194 and 3070 cm^{-1} belong to the –NH group, while the peak at 1652 cm^{-1} belongs to the C=O group (Zhou et al., 2020). It can be seen from the spectrum of CL-PA ionic liquid that the –NH group peaks of CL disappeared and the carbonyl peak of CL at 1652 cm^{-1} shifted to a lower frequency, that is, 1604 cm^{-1}, due to the bonding of a hydrogen of PA to the

nitrogen in CL (Naiyl et al., 2021). In the ionic liquid structure, the characteristic peaks of PA appear to be preserved.
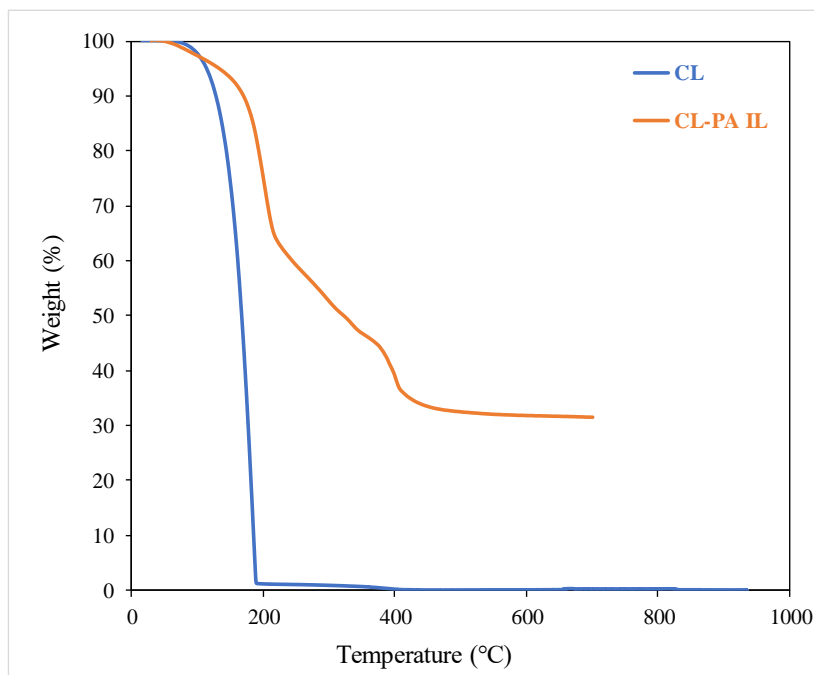

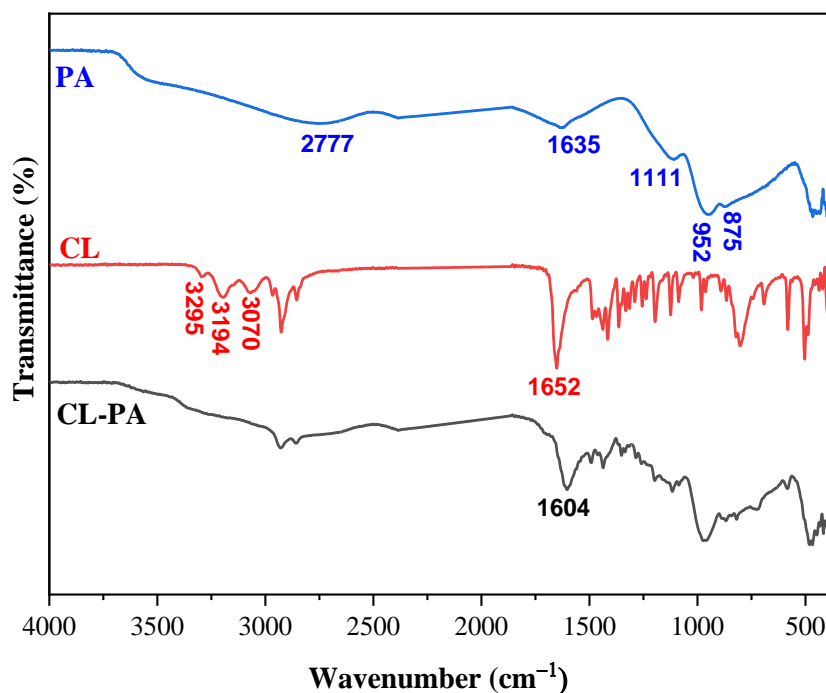**Figure 3.** Thermal stability of CL-PA ionic liquid and CL.

Figure 4. FTIR spectrum of PA, CL and CL-PA ionic liquid.

3.4. Raman Analysis

Raman analysis of CL-PA ionic liquid was carried out using a Renishaw In Via Qontor model spectrometer in the range of 4000-100 cm^{-1}. In Figure 5, in the PA spectrum, the sharp and strong band at 913 cm^{-1} (P–O) and the weak and broad bands at 354 and 491 cm^{-1} are the characteristic bands belonging to concentrated orthophosphoric acid (J. Li et al., 2011). The weak band at 1312 cm^{-1} belongs to the phosphoryl group (stretching vibration of P=O) (Cheremisina et al., 2015; Larkin, 2011) and the band at 1603 cm^{-1} belongs to the H–OH bending vibration, indicating the presence of water (Frost et al., 2013). In the CL spectrum, the bands at 584, 701, 1495 and 1641 cm^{-1} are assigned to the asymmetric C=O bending vibration, N–H stretching vibration, C–N stretching vibration and C=O stretching vibration, respectively (Naiyl et al., 2021).

171

When the spectrum of CL-PA ionic liquid was examined, the wavenumbers and the peak intensities (consequently, peak areas) of the relevant peaks belonging to 85% PA solution and CL changed. In addition, the bands at 584 and 1641 cm^{-1} belonging to CL do not appear in CL-PA ionic liquid. All these changes are an indication of the formation of a bond between CL and PA.
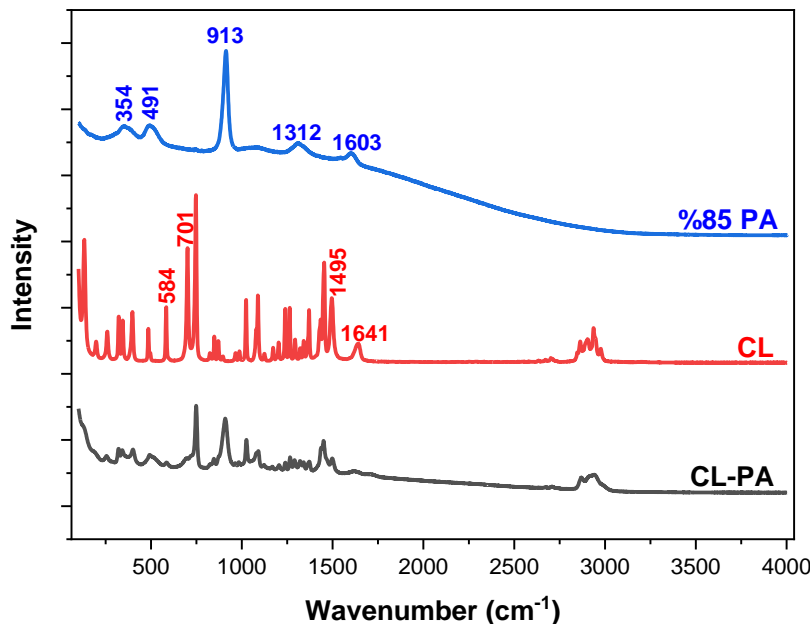

Figure 5. Raman spectrum of PA, CL and CL-PA ionic liquid.

3.5. UV-Vis Spectroscopy

UV-Vis spectra of CL-PA ionic liquid and CL were obtained in the wavelength range of 190-1100 nm using deuterium and tungsten lamps by Perkin-Elmer Lambda 35 UV-Vis spectrophotometer. For UV-Vis spectrum, CL and CL-PA were dissolved in water to be 0.5 mM. As shown in Figure 6, CL gave a maximum absorbance at 200 nm. In the spectrum of CL-PA ionic liquid, the maximum absorbance of CL at 200 nm shifted to a shorter wavelength (197 nm) due to the decrease in the electron density of the CL molecule.
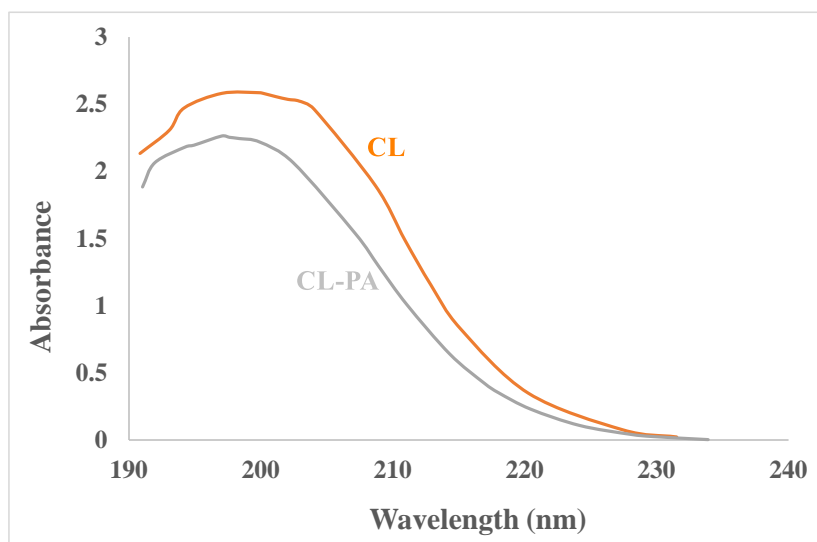

Figure 6. UV-Vis spectrum of CL-PA ionic liquid and CL.

4. OUTLOOK

Protic ionic liquids are formed by a neutralization reaction between acid and base through proton transfer (Shiflett, 2020) and therefore CL-PA is a protic ionic liquid. This water-soluble ionic liquid can be used in the removal of sulfur from fuels and the absorption of acidic flue gases. Particularly in heterogeneous reactions, mass transfer is important for reaction conversion and high viscosity at relatively low temperatures can cause trouble. For this reason, accelerating mass transfer by increasing

the reaction temperature may favor the reaction conversion. On the other hand, when increasing the temperature, it is necessary to consider the decomposition temperature of the reactants and whether the reaction is exothermic or endothermic. The reusability of the ionic liquid after reactions is also of great importance in terms of cost. It should be evaluated how many times the ionic liquid can be reused in reactions without losing its effectiveness. Moreover, ionic liquid should not dissolve in the other phase, thus leading to loss of ionic liquid. The protic ionic liquid to be used should be stored in tightly closed, leak-proof containers as it may be sensitive to air and moisture. Ionic liquid can also be used as an antimicrobial agent, but its toxic effect must be evaluated. Besides, ionic liquids with high biodegradability and low toxicity can be preferred to minimize waste from an environmental perspective. Protic ionic liquids (PILs) can be used in four main applications (Bailey et al., 2024): Catalytic transformations (due to their ability to act as solvents and catalysts and their easy separation after reactions), biomass processing (due to their power to fractionate and dissolve biomass), energy storage and conversion (due to their negligible volatility unlike that of organic solvents, high thermal stability, and high ionic conductivity), and electrocatalysis (due to the efficient modulation of electrochemical reactivity of PIL electrolytes by changing anion and cation of PIL). CL-PA ionic liquid may have the potential to be used in the above-mentioned applications of protic ionic liquids. Based on its thermal stability, it may be used as catalyst in reactions, a thermal transfer fluid, and an electrolyte in fuel cells, at temperatures below about 163 ℃.

5. CONCLUSION

It was observed that the synthesized CL-PA ionic liquid was stable in liquid state at room temperature, and the glass transition temperature was determined to be −27 ℃ from DSC analysis. Additionally, it was revealed that the thermal decomposition of protic ionic liquid CL-PA occurred in three stages. Therefore, CL-PA ionic liquid has different physicochemical properties from the starting materials CL and PA. To prove the formation of ionic liquid, UV-Vis, Raman and FTIR analyzes were performed. The three spectroscopic analyses demonstrate that a bond was formed between CL and PA according to the inspected spectra. The synthesized CL-PA protic ionic liquid may have many potential applications, such as recovery of valuable metals from waste batteries, use as electrolyte and catalyst in reactions and use as an extractant.

6. CONFLICT OF INTEREST

There is no conflict of interest to declare.

7. REFERENCES

Ashurst, P. R. (Ed.). (2016). *Chemistry and Technology of Soft Drinks and Fruit Juices*. Wiley. https://doi.org/10.1002/9781118634943

Bailey, J., Byrne, E. L., Goodrich, P., Kavanagh, P. and Swadźba-Kwaśny, M. (2024). Protic ionic liquids for sustainable uses. *Green Chem.*, *26*(3), 1092–1131. https://doi.org/10.1039/D3GC03297C

Bajpai, P. (2021). *Deep Eutectic Solvents for Pretreatment of Lignocellulosic Biomass*. Springer Singapore. https://doi.org/10.1007/978-981-16-4013-1

Cao, S., Ma, Y., Yang, L., Lin, L., Wang, J., Xing, Y., Lu, F., Cao, T., Zhao, Z. and Liu, D. (2023). Designing Low-Cost, Green, and Recyclable Deep Eutectic Solvents for Selective Separation and Recovery of Valuable Metals from Spent Li-Ion Batteries. *ACS Sustain. Chem. Eng.*, *11*(48), 16984–16994. https://doi.org/10.1021/acssuschemeng.3c04802

Celik, S., Albayrak, A. T., Akyuz, S., Ozel, A. E. and Sigirci, B. D. (2021). Synthesis, antimicrobial activity, molecular docking and ADMET study of a caprolactam-glycine cluster. *J Biomol. Struct. Dyn.*, *39*(7), 2376–2386. https://doi.org/10.1080/07391102.2020.1748112

Chen, H., Li, W., Wang, J., Xu, H., Liu, Y., Zhang, Z., Li, Y. and Zhang, Y. (2019). Adsorption of cadmium and lead ions by phosphoric acid-modified biochar generated from chicken feather: Selective adsorption and influence of dissolved organic matter. *Bioresour. Technol.*, *292*. https://doi.org/10.1016/j.biortech.2019.121948

Cheremisina, O. V., Sergeev, V. V., Chirkst, D. E. and Litvinova, T. E. (2015). Thermodynamic investigation into extraction of cerium(III) by tributyl phosphate from phosphoric acid solutions. *Russ. J. Non-ferrous Metals*, *56*(6), 615–621. https://doi.org/10.3103/S1067821215060036

Cherkasova, E. V., Patrakov, Y. F., Tryasunov, B. G., Cherkasova, T. G. and Tatarinova, E. S. (2009). Thermal analysis of rare-earth metal(III) hexa(isothiocyanato)chromate(III) complexes with ε-caprolactam. *Russ. J. Inorg. Chem.*, *54*(10), 1625–1629. https://doi.org/10.1134/S0036023609100192

Chu, G., Zhao, J., Huang, Y., Zhou, D., Liu, Y., Wu, M., Peng, H., Zhao, Q., Pan, B. and Steinberg, C. E. W. (2018). Phosphoric acid pretreatment enhances the specific surface areas of biochars by generation of micropores. *Environ. Pollut.*, *240*, 1–9. https://doi.org/10.1016/j.envpol.2018.04.003

Fang, X., Wyatt, T., Shi, J. and Yao, D. (2018). Fabrication of high-strength polyoxymethylene fibers by gel spinning. *J. Mater. Sci.*, *53*(16), 11901–11916. https://doi.org/10.1007/s10853-018-2410-5

Frost, R. L., Xi, Y., Scholz, R., Belotti, F. M. and Cândido Filho, M. (2013). Infrared and Raman spectroscopic characterization of the borate mineral colemanite – CaB3O4(OH)3·H2O – implications for the molecular structure. *J. Mol. Struct.*, *1037*, 23–28. https://doi.org/10.1016/j.molstruc.2012.11.047

Gilmour, R. (2014). *Phosphoric Acid: Purification, Uses, Technology, and Economics*. CRC Press. https://doi.org/10.1201/b16187

Guo, B., Duan, E., Zhong, Y., Gao, L., Zhang, X. and Zhao, D. (2011). Absorption and oxidation of H2S in caprolactam tetrabutyl ammonium bromide ionic liquid. *Energ. Fuel.*, *25*(1), 159–161. https://doi.org/10.1021/ef1012006

Hao, L., Su, T., Hao, D., Deng, C., Ren, W. and Lü, H. (2018). Oxidative desulfurization of diesel fuel with caprolactam-based acidic deep eutectic solvents: Tailoring the reactivity of DESs by adjusting the composition. *Cuihua Xuebao/Chinese J. Catal.*, *39*(9), 1552–1559. https://doi.org/10.1016/S1872-2067(18)63091-8

House, J. E. (2020). *Inorganic chemistry*. Academic Press.

Ichihashi, H., Ishida, M., Shiga, A., Kitamura, M., Suzuki, T., Suenobu, K. and Sugita, K. (2003). The Catalysis of Vapor-Phase Beckmann Rearrangement for the Production of ε-Caprolactam. *Catal. Surv. Asia*, *7*(4), 261–270. https://doi.org/10.1023/B:CATS.0000008165.80991.05

Kabo, G. J., Kozyro, A. A., Krouk, V. S., Sevruk, V. M., Yursha, I. A., Simirsky, V. V and Gogolinsky, V. I. (1992). Thermodynamic properties of 6-aminohexanoic lactam (-caprolactam). *J. Chem. Thermodyn.,* 24(1), 1-13. https://doi.org/10.1016/S0021-9614(05)80249-6

Kalinová, J. P., Tříska, J., Vrchotová, N. and Novák, J. (2016). Uptake of caprolactam and its influence on growth and oxygen production of Desmodesmus quadricauda algae. *Environ. Pollut.*, *213*, 518–523. https://doi.org/10.1016/j.envpol.2016.03.024

Karibayev, M. and Shah, D. (2020). Comprehensive Computational Analysis Exploring the Formation of Caprolactam-Based Deep Eutectic Solvents and Their Applications in Natural Gas Desulfurization. *Energ. Fuel.*, *34*(8), 9894–9902. https://doi.org/10.1021/acs.energyfuels.0c01721

Lange, N. A. and Speight, J. G. (2005). *Lange's handbook of chemistry.* McGraw-Hill.

Larkin, P. (2011). *Infrared and Raman Spectroscopy*. Elsevier. https://doi.org/10.1016/C2010-0-68479-3

Li, J., Zhang, C. and Luo, J. (2011). Superlubricity behavior with phosphoric acid-water network induced by rubbing. *Langmuir*, *27*(15), 9413–9417. https://doi.org/10.1021/la201535x

Li, W.-C., Lu, A.-H., Palkovits, R., Schmidt, W., Spliethoff, B. and Schüth, F. (2005). Hierarchically Structured Monolithic Silicalite-1 Consisting of Crystallized Nanoparticles and Its Performance in the Beckmann Rearrangement of Cyclohexanone Oxime. *J. Am. Chem. Soc.*, *127*(36), 12595–12600. https://doi.org/10.1021/ja052693v

Liu, B., Zhao, J. and Wei, F. (2013). Characterization of caprolactam based eutectic ionic liquids and their application in SO₂ absorption. *J. Mol. Liq.*, *180*, 19–25. https://doi.org/10.1016/j.molliq.2012.12.024

Malek, M. A. and Chong, C. S. (2000). FTIR study of H₂O in polyallyl diglycol carbonate. *Vib. Spectrosc.,* 24, 181-184. https://doi.org/10.1016/S0924-2031(00)00071-0

Benvenuto, M. A. and Plaumann, H. (2021). Industrial Catalysis. Walter de Gruyter GmbH, Berlin/Boston.

Mather, R. R. and Wardman, R. H. (2015). *The chemistry of textile fibres*, 2nd Edition, The Royal Society of Chemistry. https://doi.org/10.1039/9781782626534

Maxwell, G. R. (2005). *Synthetic Nitrogen Products*. Kluwer Academic Publishers. https://doi.org/10.1007/b106641

McGraw-Hill Concise Encyclopedia of Science and Technology FIFTH EDITION. (2005). McGraw-Hill Companies, Inc.

Naiyl, R. A., Kengara, F. O., Kiriamiti, K. H. and Ragab, Y. A. (2021). Synthesis and Characterization of Caprolactam- based Ionic Liquids as Green Solvents. *Asian J. Appl. Chem. Res.*, 74–87. https://doi.org/10.9734/ajacr/2021/v8i430201

Naiyl, R. A., Kengara, F. O., Kiriamiti, K. H. and Ragab, Y. A. (2022). Lipid extraction from microalgae using pure caprolactam-based ionic liquids and with organic co-solvent. *PeerJ Anal. Chem.*, *4*, e13. https://doi.org/10.7717/peerj-achem.13

Płotka-Wasylka, J., de la Guardia, M., Andruch, V. and Vilková, M. (2020). Deep eutectic solvents vs ionic liquids: Similarities and differences. *Microchem. J.,* 159, 105539. https://doi.org/10.1016/j.microc.2020.105539

Ren, C., Wang, Z., Gao, Q., Li, J., Jiang, S., Huang, Q., Yang, Y., Zhang, J., Wang, Y., Hu, Y., Liu, Z. and Guo, X. (2023). Novel Brønsted Acidic Ionic Liquids as High Efficiency Catalysts for Liquid-Phase Beckmann Rearrangement. *Catalysts*, *13*(6). https://doi.org/10.3390/catal13060978

Sato, M., Ikushima, Y., Hatakeda, K. and Ikeshoji, T. (2005). Acceleration of Chemical Reactions Using a Supercritical Water Microreaction System. *Int. J. Chem. React. Eng.*, *3*(1). https://doi.org/10.2202/1542-6580.1294

Shiflett, M. B. (Ed.). (2020). *Commercial Applications of Ionic Liquids*. Springer International Publishing. https://doi.org/10.1007/978-3-030-35245-5

Sun, Q., Lin, D., Khayatnezhad, M. and Taghavi, M. (2021). Investigation of phosphoric acid fuel cell, linear Fresnel solar reflector and Organic Rankine Cycle polygeneration energy system in different climatic conditions. *Process Saf. Environ.*, *147*, 993–1008. https://doi.org/10.1016/j.psep.2021.01.035

Sun, S., Liu, S., Yu, F., Zhang, J., Xing, W. and Yu, S. (2022). Reusable Deep Eutectic Solvents for Clean ε-Caprolactam Synthesis under Mild Conditions. *ACS Sustain. Chem. Eng.*, *10*(4), 1675–1688. https://doi.org/10.1021/acssuschemeng.1c07613

Wang, H., Qin, M., Wu, Q., Cheng, D. G., Meng, X., Wang, L. and Xiao, F. S. (2023). Zeolite Catalysts for Green Production of Caprolactam. *Ind. Eng. Chem. Res.,* 62(5), 2217–2224. https://doi.org/10.1021/acs.iecr.2c01693

Wang, L. K. (2006). *Waste treatment in the process industries*. CRC/Taylor and Francis.

Wang, S., Liu, G., Wan, W., Li, X., Li, J. and Wang, C. (2024). Acetamide-Caprolactam Deep Eutectic Solvent-Based Electrolyte for Stable Zn-Metal Batteries. *Adv. Mater.*, *36*(5). https://doi.org/10.1002/adma.202306546

Wei, H., Wang, T., Zhang, Q., Jiang, Y. and Mo, C. (2020). Study of composition and structure of aluminum phosphate binder. *J. Chin. Chem. Soc.*, *67*(1), 116–124. https://doi.org/10.1002/jccs.201900008

Xu, C., Zhang, W., Li, P., Zhao, S., Du, Y., Jin, H., Zhang, Y., Wang, Z. and Zhang, J. (2019). High-performance aluminum-ion batteries based on AlCl3/caprolactam electrolytes. *Sustain. Energ. Fuels*, *4*(1), 121–127. https://doi.org/10.1039/c9se00941h

Xu, L., Yin, J., Luo, Y., Liu, H., Li, H., Zhu, L., He, J., Jiang, W., Zhu, W. and Li, H. (2022). Rational Design of Caprolactam-Based Deep Eutectic Solvents for Extractive Desulfurization of Diesel Fuel and Mechanism Study. *ACS Sustain. Chem. Eng.*, *10*(14), 4551–4560. https://doi.org/10.1021/acssuschemeng.1c08413

Yang, H., Jiang, B., Sun, Y., Hao, L., Huang, Z. and Zhang, L. (2016). Synthesis and oxidative desulfurization of novel lactam-based Brønsted-Lewis acidic ionic liquids. *Chem. Eng. J.*, *306*, 131–138. https://doi.org/10.1016/j.cej.2016.07.044

Yankova, R. and Tankov, I. (2021). Hydrogen bonding effect on the thermal behavior of acidic ionic liquids. *J. Mol. Struct.*, *1238*, 130416. https://doi.org/10.1016/j.molstruc.2021.130416

You, K., Mao, L., Yin, D., Liu, P. and Luo, H. (2008). Beckmann rearrangement of cyclohexanone oxime to ε-caprolactam catalyzed by sulfonic acid resin in DMSO. *Catal. Commun.*, *9*(6), 1521–1526. https://doi.org/10.1016/j.catcom.2008.01.011

Zhang, Y., Cui, P., Luo, G., Chen, L., Li, X., Chao, Y. and Zhu, W. (2023). One-step selective separation and efficient recovery of valuable metals from spent lithium batteries by phosphoric acid-based deep eutectic solvent. *Green Chem. Eng.*, *5*(3), 390-398. https://doi.org/10.1016/j.gce.2023.10.002

Zhou, Q., Yu, Y., Liu, Q., Zhuang, Y., Lv, Y., Song, N. and Ni, L. (2020). Morphology evolution and thermodynamic behavior of the "soft core hard shell" structure formed by reactive amino triblock in epoxy resin. *J. Mater. Sci.*, *55*(35), 16846–16859. https://doi.org/10.1007/s10853-020-05258-2

Zhu, Z., Luo, X., Sokolov, A. P., Sokolov, A. P. and Paddison, S. J. (2020). Proton Transfer in Phosphoric Acid-Based Protic Ionic Liquids: Effects of the Base. *J. Phys. Chem. A*, *124*(20), 4141–4149. https://doi.org/10.1021/acs.jpca.0c02863